Regular Article

Sulfur Dioxide Internal and External Adsorption on the Single-Walled Carbon Nanotubes: DFT Study

M. Oftadeh[a,*], M. Gholamian[a] and H.H. Abdallah[b]

[a]Chemistry Department, Payame Noor University, 19295-4697 Tehran, I. R. of Iran
[b]Department of Chemistry, Education College, Salahaddin University, Erbil, Iraq

(Received 1 September 2013, Accepted 28 December 2013)

Density functional theory is used to investigate sulfur dioxide physisorption inside and outside of single-walled carbon nanotube (SWCNT) of (5,0) and (5,5). This study is conducted at B3LYP/6-31G* level of theory. Sulfur dioxide molecule is studied with axis oriented parallel or perpendicular to the nanotube wall. Both internal and external adsorption on nanotubes are increased with the angle of interaction being at maximum of 90° to the tube axis. The harmonic frequencies are computed from analytical derivatives for all species in order to define the minimum energy structures. The lowest values of HOMO and LUMO energies are obtained in the process of the adsorption on the external wall of (5,5) nanotube. The dipole moment of the SWCNTs-SO_2 system is highly increased and is more than that of SWCNTs- H_2S and SWCNTs- CO_2. The lowest ΔG_{tot} for SO_2 on the outside wall of (5,0) is obtained while this quantity is positive and is not a favorable adsorption process for H_2S on the nanotubes. The NBO analysis shows the change in the electronic structure of nanotubes could be suitable for fabricating sensors.

INTRODUCTION

Environment is a complex and large collection of various factors that contribute to the process of evolution of organisms and their components. Human activities affect on it. Industrial development and population growth increase the consumption of resources and energy [1]. Approximately, 100 million tons of sulfur is entered into the atmosphere by human activities mostly originating from the rock and petroleum fuels [2,3]. Sulfur oxides and suspended particles in the air have severe effects on humans and the environment if the relative humidity is high. One of the costly effects of sulfur dioxide pollutant is deterioration of building materials. In recent years, due to the high risks associated with the presence of SO_2 and its emission in the environment including acid rain, many different processes have been employed to remove these contaminants.

Carbon nanotubes have been used to adsorb pollutant gases. They have ultra high mechanical [5-7], electrical [5-8], and thermal conductivity [8-10], the aspect ratio (length/

diameter) and low density [11]. A lot of theoretical and experimental researches have been done for the adsorption of gases such as O_2 [12-14], NO [15], CO_2 [16], S [17], CO [18, 20], H_2 [19], on nanotubes. The results have shown that adsorption of SO_2 on thin film of SWCNTs can be used as a chemical sensor in the nanometer scale devices [21].

The adsorption and desorption behaviors of SO_2 onto activated carbons prepared from pistachio-nut shells were studied theoretically and experimentally in a fixed bed column [22]. A mathematical model for a single gas adsorbate on a fixed-bed system was derived and solved by a finite-difference method. The experimental data showed that the breakthrough time is decreased with increasing feed concentration, flow rate and temperature. The trends were correctly predicted by the model calculations.

The adsorption of three types of gas molecules (SO_2, CH_3OH and CH_4) onto Pd-doped (5,5) SWCNTs has been studied within DFT [23]. The Pd-SWCNTs can be utilized as good sensors for these gases due to large electron charge transfer and strong binding energy between the Pd-SWCNTs and these molecules. The adsorption features of the gases are different. The interaction between CH_4 and the

_____
*Corresponding author. E-mail: moftadeh@pnu.ac.ir

Pd-SWCNT is an electrostatic one and a bound complex of $(Pd-SWCNT)-(CH_4)^+$ is formed due to charge transfer between them, while the adsorption of CH_3OH and SO_2 onto the Pd-SWCNTs is attributed to physical and chemical adsorption, respectively.

Humidity-assisted desorption of SO_2 and NO_2 has been experimentally investigated on carbon nanotubes [24]. The results have shown that the resisted desorption of SO_2 on carbon nanotubes in dichloroethane solution increases at high humidity level (92%) and no charge is observed in low humidity level, while there is no change in desorption of NO_2 in a different level of humidity either.

The electronic properties of a nanotube upon adsorption of gas molecules including NO_2, O_2, NH_3, N_2, H_2O, Ar, *etc*. on carbon nanotube were demonstrated using first principles methods [25]. All molecules were weakly adsorbed on SWCNT with a small charge donor or an accepter of the nanotube. The adsorption of some gas molecules on SWCNTs can cause a significant change in electronic and transport properties of the nanotube due to the charge transfer and charge fluctuation.

The effective parameters of (5,0) and (5,5) SWCNTs during the interaction with CO_2 and H_2S as sensors were determined [26,27] by DFT at the B3LYP level of theory. The carbon dioxide molecule was predicted to bind only weakly to nanotubes, and the tube-molecule interactions could be identified as physisorption. CO_2 adsorption was stronger on the external walls than that on the internal walls, and adsorption on the external wall of (5, 0) was stronger than that on the external wall of (5, 5); the adsorption energies are exothermic. H_2S molecule adsorption on the internal and external wall of (5,0) nanotube was chemical and physical adsorption, respectively. The most favorable adsorption distance from the molecule to the external walls of (5,0) and (5,5) SWCNTs was 2.6 and 2.8 Å, respectively. The results of the thermodynamic quantities certified no simultaneous H_2S adsorption process, while the NBO analysis showed the change in the electronic structure of nanotubes which could be suitable for fabricating sensors. In this paper, the probability of the adsorption of SO_2 on the SWCNTs for the removal of the gas from the environment is theoretically investigated.

Method

In the present study, the interaction of sulfur dioxide with single-wall carbon nanotube of (5,0) and (5,5) was investigated at B3LYP/6-31G(d) level of theory. Computational calculations were performed in the gaseous phase by the Linux version of Gaussian 09 with 32 processors *via* shared memory [28]. Figure 1 shows the optimized geometry of the combined systems. The harmonic frequencies were computed from analytical derivatives for all species in order to define the minimum-energy structures. The geometry of all molecules under investigation was determined by optimizing all geometrical variables without any symmetry constraints. For both the external and internal cases, the effect of molecular orientation on the adsorption process was studied. The adsorption energies, the thermodynamic properties, HOMO-LUMO energy gaps and partial charges of the interacting atoms were also studied.

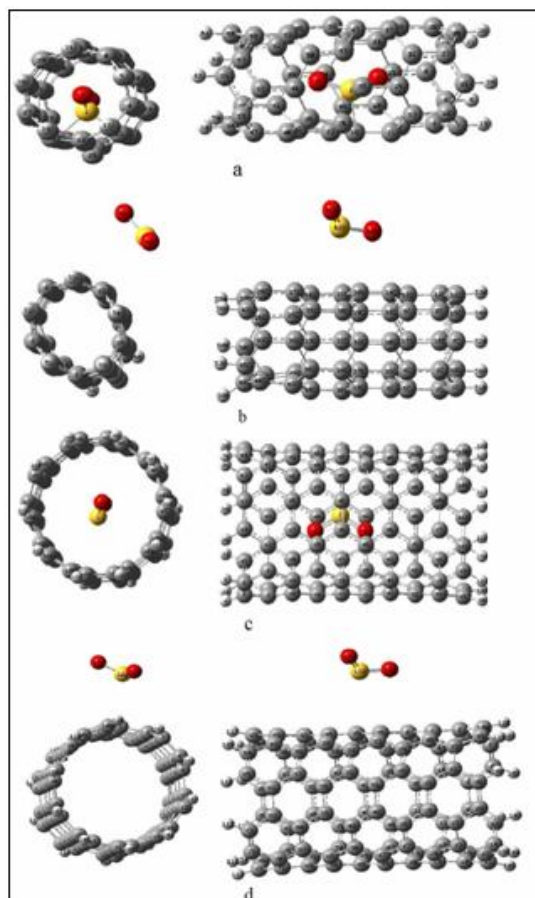The (5,0) SWCNT containing 50 carbon atoms of length

Fig. 1. Optimized molecular geometry and the interaction between SO_2-(5,0) (a, b) and SO_2-(5,5) (c, d).

8.5 Å and diameter 4 Å, saturated with 10 hydrogen atoms, and the (5,5) SWCNT containing 100 carbon atoms of length 9.8 Å and diameter of 6.85 Å were saturated with 20 hydrogen atoms and selected for this purpose. The calculated parameters, the energy interaction, E_{ads}, of SO_2 with the inside wall of SWCNT of (5,0) and (5,5), were obtained through the following formula:

$$E_{ads} = E_{SO2\text{-}nanotube} - (E_{nanotube} + E_{SO2}) \tag{1}$$

where $E_{SO2\text{-}nanotube}$ is the total energy of the optimized nanotube-SO_2 system, $E_{nanotube}$ is the total energy of the optimized nanotube and E_{SO2} is the total energy of the isolated SO_2 molecule. Given this, $E_{ads} < 0$ corresponds to exothermic adsorption, leading to a stable structure.

$$\Delta G_{tot} = \Delta G_{SO2\text{-}SWCNT} - (\Delta G_{nanotube} + \Delta G_{SO2}) \tag{2}$$

Total zero point energy, total internal energy, and total enthalpy were calculated by the same formula.

RESULTS AND DISCUSSION

Energy Calculations

The optimized molecular geometry and the interaction between (5,0) SWCNT-SO_2 and (5,5) SWCNT-SO_2 are presented in Fig. 1. As can be seen, the SO_2 is chemically adsorbed on the internal wall of the (5,0) nanotube while it is physically adsorbed on the external wall of (5,0) and both internal and external walls of (5,5) nanotubes. Figure 2 schematically represents the vertical (a,b,c) and the
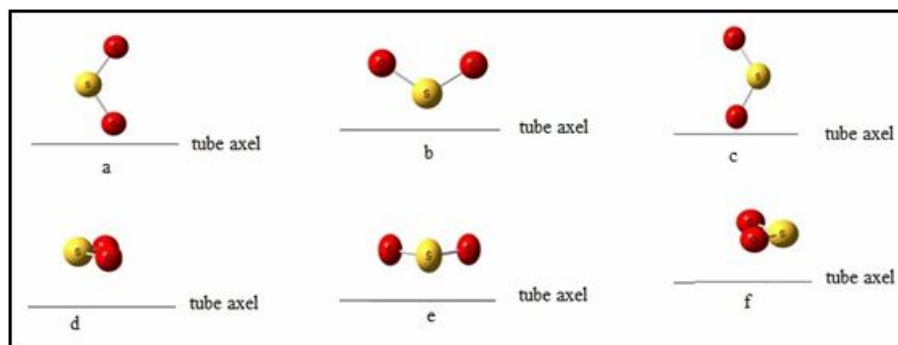

Fig. 2. Schematic representation of the vertical (a, b, c) and the horizontal (d, e, f) rotations around the tube axle.
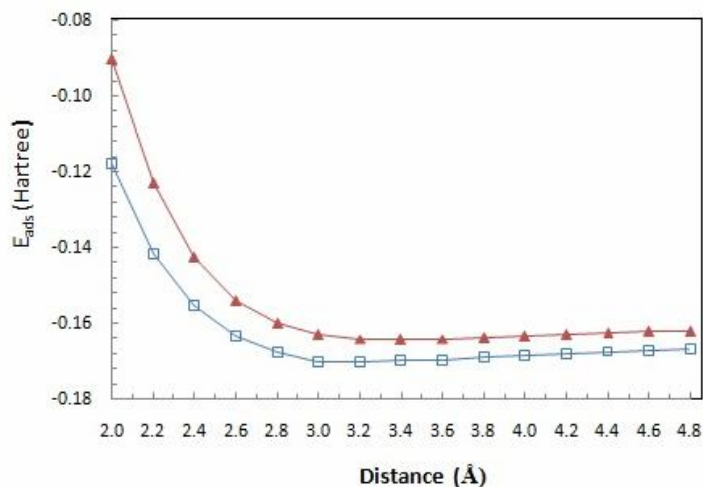

Fig. 3. The effect of different distances of SO_2 on the external SWCNT, adsorption energy of (5,0) -SO_2 (□) and adsorption energy of (5,5) -SO_2 (▲), as calculated by B3LYP/6-31G*.

horizontal (d, e, f) rotations around the tube axle. Figure 3 shows the effect of the distances of the SO_2 molecule on the adsorption energies calculated by B3LYP/6-31G*.

The most favorable adsorption distances between the molecule and external wall nanotubes of the (5,0) and (5,5) were 3.0, and 3.4 Å, respectively. Figures 4 and 5 show that the adsorption energy increases with the angle of interaction, reaching a maximum at 90° too. The basis set
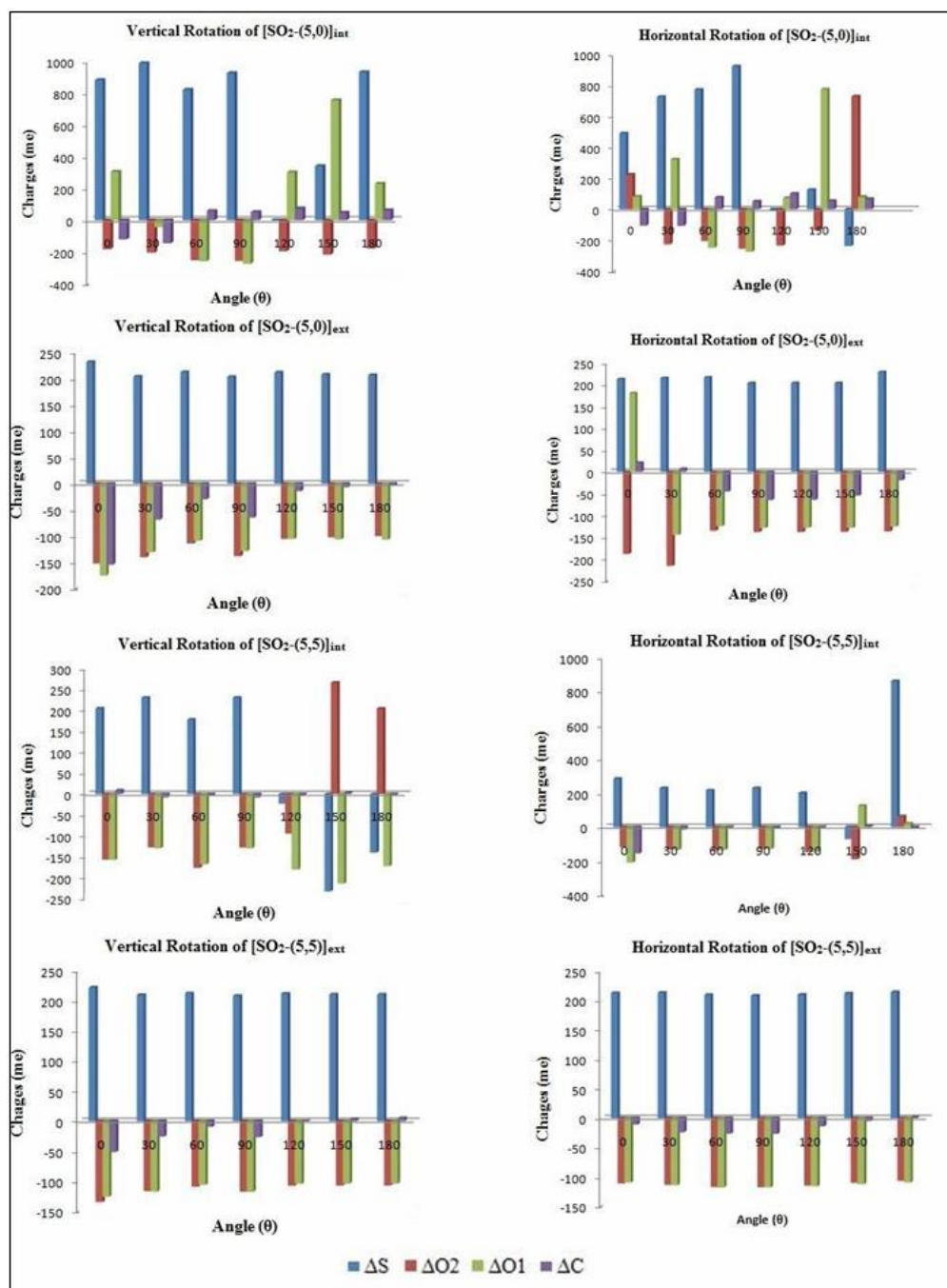

Fig. 4. The difference in partial natural charges on S, O1, O2 and C atoms of the entitled systems after and before adsorption during the vertical and horizontal rotations of the SO_2 molecule along the nanotube.

33

superposition errors (BSSE) have been estimated for the counterpoise correction [29] and their effects on the energy changes during the rotation of SO_2 molecule around the tube axle for the internal and external nanotubes have been

calculated. In Table 1, the calculated parameters such as adsorption energy (E_{ads}), BSSE, E_{ads}^{BSSE}, HOMO, LUMO, the gap energy, and the dipole moment in the adsorption process of SO_2 molecule on the internal and external walls
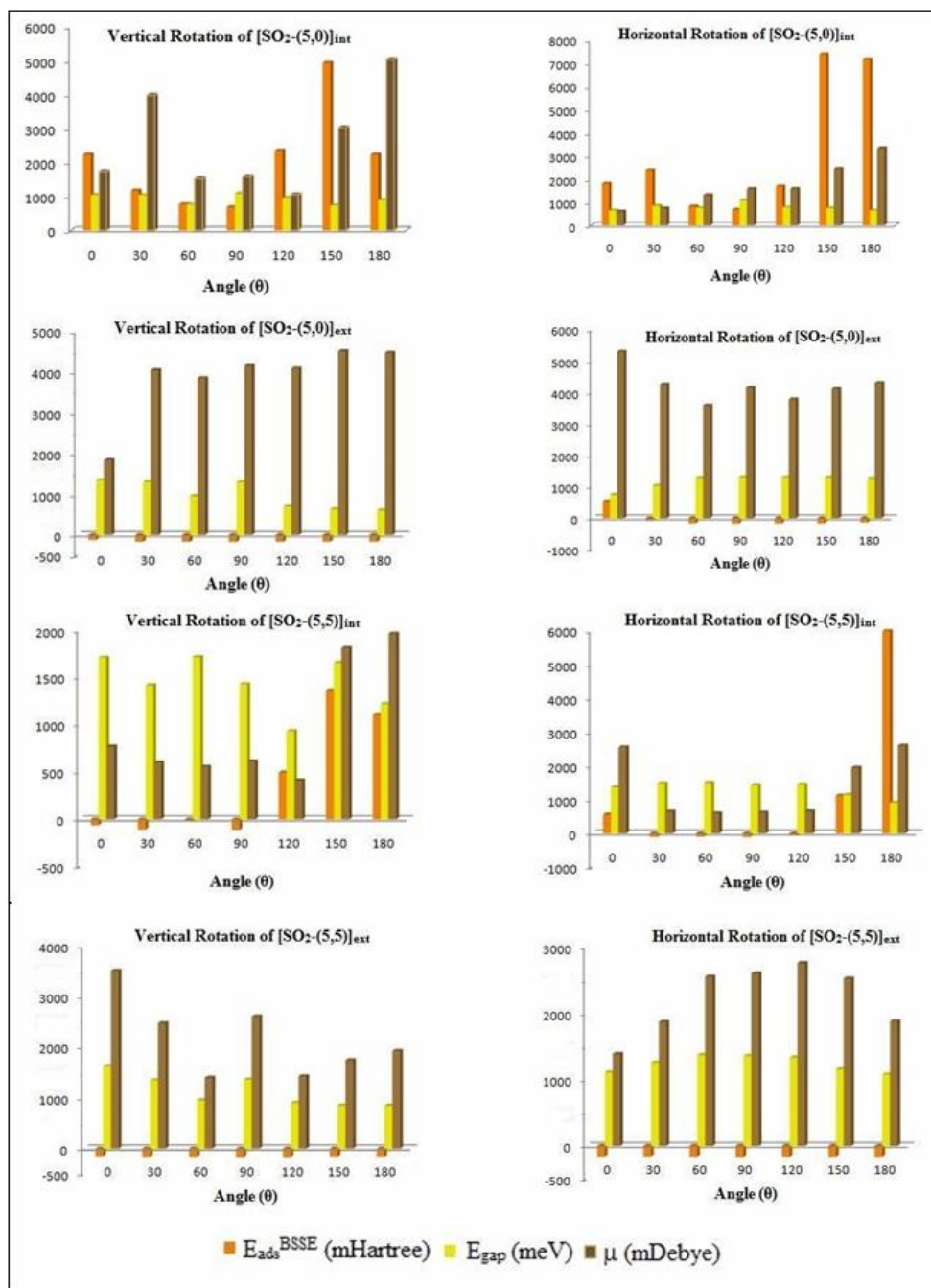

Fig. 5. Variation of E_{ads}^{BSSE}, E_{gap} and μ of the entitled systems during the vertical and horizontal rotation of the SO_2 molecule along the nanotube.

Table 1. Effect of Both Adsorption of SO_2 Molecule on the Optical Parameters of the Systems Adsorption Energy (E_{ads}), BSSE, E_{ads}^{BSSE}, HOMO, LUMO (in Hartree), Gap Energy (in eV), Dipole Moment, μ, (in Debye), in the Adsorption Process of SO_2 Molecule on the Internal and External Walls of (5,0) and (5,5) Nanotubes Calculated by B3LYP/6-31G*

Optimized systems	E_{ads}	BSSE	E_{ads}^{BSSE}	HOMO	LUMO	E_{gap}	μ
(5,0)	-	-	-	-0.1763	-0.1126	1.7326	0.0
(5,5)	-	-	-	-0.1591	-0.0963	1.7082	0.0
$[SO_2-(5,0)]_{int}$	0.6653	0.0250	0.6903	-0.1458	-0.1059	1.0853	1.5868
$[SO_2-(5,0)]_{ext}$	-0.1711	0.0016	-0.1695	-0.1608	-0.1129	1.3029	4.1514
$[SO_2-(5,5)]_{int}$	-0.1205	0.0099	-0.1106	-0.1594	-0.0963	1.4333	0.6132
$[SO_2-(5,5)]_{ext}$	-0.1656	0.0007	-0.1666	-0.1619	-0.1120	1.3600	2.6061

of (5,0) and (5,5) nanotubes are collected. According to the results, adsorption of SO_2 molecule on the external wall of the nanotube is more effective than that on the internal wall. The adsorption of SO_2 on the external wall of the (5,0) nanotube is more effective than that on the external wall of the (5,5) nanotube, while on the internal wall of the (5,5) nanotube is more effective than the internal wall of the (5,0) nanotube. The values of BSSE are very low, indicating the convenient bases set for the complex system. The energy gap is decreased after the interaction of SO_2 in contrast to H_2S [27], as compared with CO_2 [26]. The lowest values of HOMO and LUMO energies are obtained in the process of the adsorption on the external wall of (5,5) nanotube. The dipole moment of the SWCNTs-SO_2 system is highly increased and is more than SWCNTs-H_2S and SWCNTs-CO_2.

NBO Calculations

Natural bond orbital calculations have been performed for all the rotations in order to calculate the charge difference before and after adsorption of SO_2 molecule on nanotubes. The charge of S and O atoms before adsorption is 1.559 and -0.778, respectively. The partial charge differences on the interaction of atoms including sulfur

atom, oxygen atoms and the nearest carbon atom of interaction zoon of (5,0) and (5,5) nanotubes in the presence of SO_2 molecule and in the vicinity of internal and external walls for all rotations have been shown in Fig. 4. They represent the change in the electronic structure of nanotube. They can be used as a response of the adsorption in the sensor equipment.

Variation of the energy gap, the dipole moment, and the charge on atoms in the activated sites of the system during the rotation of the molecule have been shown in Fig. 5. The energy gap changes for the vertical rotation on the outside wall of (5,0) and (5,5) are more than the rest of rotations. Compared with the H_2S, the horizontal rotations on the inner wall of (5,0) and (5,5) lead to the maximum energy gap changes.

Comparison of the density of states (DOS) for SWCNTs before and after the adsorption of SO_2 has been presented in Figs. 6 and 7. As can be seen, The DOS between the valance bond and conduction bond is not zero and both structures are semiconductors. The energy gap for (5,0) and (5,5) is 1.73 and 1.71 eV, respectively, representing the semiconductor ranges. It shows that the energy gap after SO_2 adsorption on the inside and outside wall of (5,0) decreases to about 0.65, 0.43 eV and for the inside and
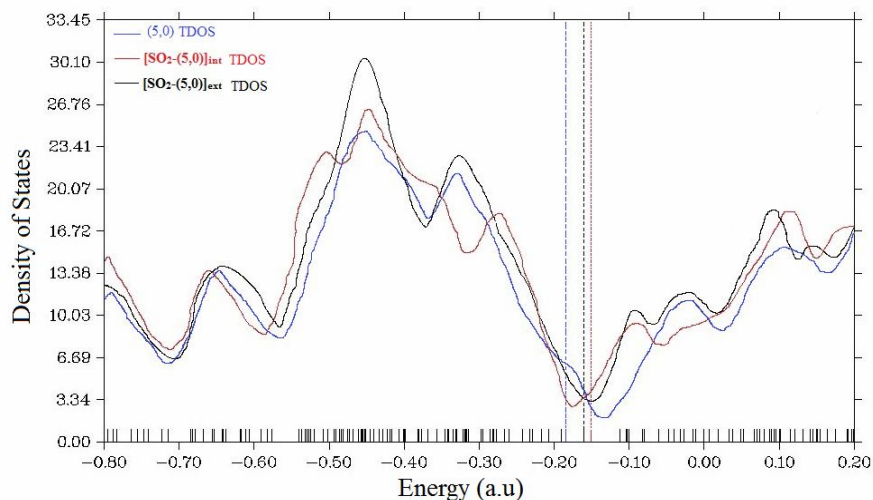
Fig. 6. Density of states (DOS) for the bare (5,0) SWCNT and the adsorbed SO_2 gas systems.
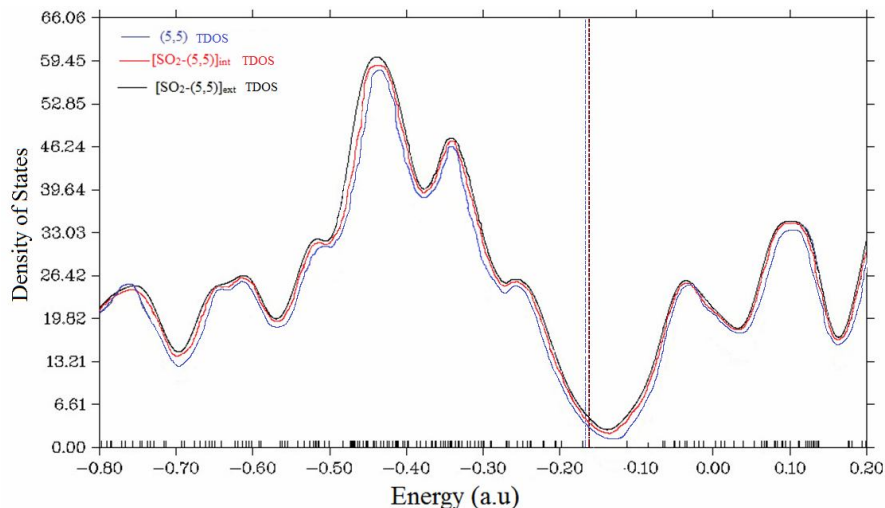

Fig. 7. Density of states (DOS) for the bare (5,5) SWCNT and the adsorbed SO_2 gas systems.

outside wall of (5,5), it decreases to about 0.28, 0.35, thereby changing the DOS in the conduction bond.

Dipole moment variations on (5,0) are more than (5,5), while these variations for H_2S are similar. The sulfur charge variations on the inner wall of (5,5) and (5, 0) are more than the outer wall, similar to H_2S. Being more than the rest of rotations, the horizontal rotation of SO_2 on the inner wall of (5,5) changes the neighbor carbon charge, while the maximum variation occurs on the inside wall of (5,0) and for the vertical rotations on the outside wall of (5,0). Such changes are not apparent for H_2S on the (5,5), and few

changes are observed for the horizontal rotations on (5,0). Variation of the oxygen charge is evident for the inner wall of (5,0) and (5,5), as much as H_2S on the inner wall of (5,0). This is not evident for H_2S inside (5,5).

Previous results for H_2S molecules [27], compared to SO_2 show the adsorption of the former is from the hydrogen atoms and the latter is from sulfur atom. The charge difference of S atom in H_2S and SO_2 is negative and positive, respectively. This is because of the electronegativity of the oxygen atoms. Because of the electron attraction toward the oxygen atoms in SO_2
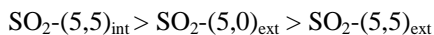
molecule, this molecule orients horizontally with respect to axial nanotube in comparison to the H_2S molecule during the adsorption. Moreover, the nanotube acts as a donor specie in the SO_2 interaction while it acts as an acceptor specie in the H_2S interaction.

The calculated values of q (in esu) and the orbital interaction energy ($\Delta E^{(2)}$) in all favorable adsorption, based on NBO analysis during the process of CT from the donor to the recipient along with the intensity of the CT interactions, are presented in Table 2, for the gas phase. The amounts of transferred partial charge between the two donor and acceptor species ($q_{donor \to acceptor}$) were calculated by the occupation numbers of NBO data for evaluating the orbital interaction energy ($\Delta E^{(2)}$) between the HOMO and LUMO of the donor-acceptor system. In a quantitative sense, the energetic effects due to these interactions may be estimated by the second-order perturbation theoretical expressions of the following form [30]:

$$q_{donor \to acceptor} \cong 2 \left(\frac{\Psi_{don}^* \left| \hat{F} \right| \Psi_{acc}^*}{\varepsilon_{acc} - \varepsilon_{don}} \right)^2 \quad (1)$$

$$\Delta E^{(2)} = 2 \frac{\left\langle \Psi_{don}^* \left| \hat{F} \right| \Psi_{acc}^* \right\rangle^2}{\varepsilon_{acc} - \varepsilon_{don}} \quad (2)$$

where F is the Fock operator, $\langle \Psi_{don}^* | F | \Psi_{acc}^* \rangle$ is the matrix element of the Fock operator between the donor and acceptor wave functions, and ε_{don} and ε_{acc} are the energies of the donor and acceptor orbitals involved in electron transfer. The stabilisation energies, $\Delta E^{(2)}$, are proportional to the NBO interacting intensities. This reveals the origin of intermolecular interactions. According to the interaction energy ($\Delta E^{(2)}$) values, loan pairs of O or S molecular orbitals of SO_2 molecule to σ^* and loan pairs of the nearest molecular orbitals of the carbon atoms in the nanotubes play the most important role. Therefore, the amounts of total charge transfer show the following trends according to the reported orbital interaction energies in Table 2:

$$SO_2\text{-}(5,5)_{int} > SO_2\text{-}(5,0)_{ext} > SO_2\text{-}(5,5)_{ext}$$

During the adsorption reactions between (5,0) or (5,5) and SO_2, Table 2 shows the calculated stabilisation energies, $\Delta E^{(2)}$. The interactions of some molecular orbitals of the two constituents in the favorable adsorption systems with the largest $\Delta E^{(2)}$ values show the more intensive interaction between donor LPs and electron acceptor bonding or antibonding orbitals considered. For $SO_2\text{-}(5,0)_{ext}$, these were mainly due to the interactions of $n_S \to \sigma_{C21\text{-}C24}^*$ and $n_{O1} \to n_{C13}$ with a total stabilisation energy of 12.08 kJ mol^{-1} and 27.58 esu for charge transfer from SO_2 to the nanotube. These donor and acceptor orbitals which took part in the stabilisation of the system were mainly p character lone pairs and p character antibonding, respectively. For the SO_2-$(5,5)_{int}$, they are mainly related to $n_S^* \to \sigma_{C57\text{-}C70}$ and $n_{O2} \to \sigma_{C57\text{-}C70}$ with a total stabilisation energy of 2.59 kJ/mol and 30.20 esu for charge transfer from SO_2 to the (5,5) nanotube and they were described as p character lone pairs and p character bonding, (p, p), for the donor and the acceptor orbitals, respectively. For the SO_2-$(5,5)_{ext}$, there is a weak interaction between the two constituents from the charge transfer point of view. The NBO analysis clearly shows that one of the contributing orbitals of the interaction was mainly p in character, convenient for CT phenomena.

Thermodynamic Parameters

Table 3 shows thermodynamic parameters including the total zero-point energy, the total internal energy, the total enthalpy, and the total Gibbs free energy in the adsorption process of SO_2 molecule on the internal and external walls of (5,0) and (5,5) nanotubes. The results show that the adsorption process is favorable on outside (5,0), and on both inside and outside (5,5). The lowest ΔG_{tot} for SO_2 on the outside wall of (5,0) is obtained while this quantity is positive and not a favorable adsorption process for H_2S on the nanotubes [27]. Comparing the results of Table 1 and Table 3 shows that there is a relationship between adsorption energies and thermodynamic energies. Total Gibbs free energies have a similar trend with the adsorption energies. This similarity is observed for other thermodynamic energies. It may be concluded that the zigzag nanotube form is more favorable for the adsorption of H_2S than the armchair nanotube form.

CONCLUSIONS

The adsorption of SO_2 molecule on the external wall of nanotube is found to be more effective than that on the internal wall while the adsorption of SO_2 on the external

Table 2. Calculated $q_{donor \to acceptor}$ Values and the Orbital Interaction Energy ($\Delta E^{(2)}$) Between the Nanotube and SO_2 Based on NBO Analysis in the Gas Phase

Optimized system	Donor→ Acceptor	$q_{donor \to acceptor}$ 10^{-3} esu	$\Delta E^{(2)}$ kJ mol^{-1}
[SO$_2$-(5,0)]$_{ext}$[a]	σ^* ... σ^*	3.67	0.75
	σ ... n	1.68	0.92
	n ... σ^*	17.15	8.28
	$n_{O1} \to n_{C13}$	10.43	3.80
	π ... σ^*	1.29	1.71
	$n_S \to \pi^*_{C21}$	0.32	1.38
[SO$_2$-(5,5)]$_{int}$[b]	n* ... σ	20.00	1.84
	n ... σ ...	10.20	0.75
	n* ... σ^*	1.52	0.79
	σ ... $\to \sigma^*$ ...	0.83	0.96
	σ ... σ^*	0.83	0.96
[SO$_2$-(5,5)]$_{ext}$[c]	σ ... $\to \pi^*$	0.15	0.29
	n* ... $\to \sigma^*$ ...	2.88	1.42
	n ... $\to \sigma^*$ ...	0.71	0.96
	$n_S \to \pi^*_{C38}$	0.12	0.50

[a]See Fig. 8 in Supplementary file. [b]See Fig. 9 in Supplementary file. [c]See Fig. 10 in Supplementary file.

wall of (5,0) is more effective than that of (5,5). On the other hand, the adsorption of SO_2 on the internal wall of (5,5) is more effective than that of (5,0).

The results showed that the maximum adsorption of SO_2 molecule occurs at 90° angle relative to nanotube axle. The most favorable adsorption distances from the molecule to the external wall of (5,0) and (5,5) are 3.0 and 3.4 Å, respectively. The thermodynamic quantities of the SO_2 adsorption process indicated that the adsorption on the internal wall of (5,0) is unfavorable, and is favorable for the external walls of (5,0) and internal and external walls of (5,5). The NBO analysis is in consistent with the

Table 3. Thermodynamic Parameters, Including Total Zero-Point Energy, ZPE, Total Internal Energy, ΔU_{tot}, Total Enthalpy, ΔH_{tot}, and Total Gibbs Free Energy, ΔG_{tot}, (in kcal mol^{-1}) in the Adsorption Process of SO_2 Molecule on the Internal and External Walls of (5,0) and (5,5) Nanotubes Calculated by B3LYP/6-31G*

Optimized systems	ZPE	ΔU_{tot}	ΔH_{tot}	ΔG_{tot}
$[SO_2-(5,0)]_{int}$	412.420	411.8910	411.3263	426.6009
$[SO_2-(5,0)]_{ext}$	-106.1102	-104.9807	-105.6082	-96.2428
$[SO_2-(5,5)]_{int}$	-73.7940	-72.8527	-73.4803	-62.4802
$[SO_2-(5,5)]_{ext}$	-102.0942	-100.7765	-101.3413	-94.3001

thermodynamic quantities, showing that the carbon nanotubes (5,0) and (5,5) are good sensors for adsorbing SO_2 molecule because of changing the electrical properties of nanostructures when exposed to the target gas analytes.

ACKNOWLEDGEMENTS

REFERENCES

[1] N.D Nevers, Air Pollution Control Engineering, McGraw-Hill, 2000.

[2] S.R. Bagheri, E. Jamshidi, A. Najafabadi, Chem. Eng. Technol. 30 (2007) 250.

[3] L. Curtis, W. Rea, P. Smith-Willis, E. Fenyves, Y. Pan, Environ. Int. 32 (2006) 815.

[4] H.S. Peavy, D.R. Rowe, G. Tchobanoglous, Environmental Engineering, McGraw-Hill, 1985.

[5] E.T. Thostenson, W.Z. Li, D.Z. Wang, Z.F. Ren, T.W. Chou, J. Appl. Phys. 91 (2002) 6034.

[6] J. Suhr, N. Koratkar, P. Keblinski, P. Ajayan, Nat. Mater. 4 (2005) 134.

[7] F.H. Gojny, M.H.G. Wichmann, U. Köpke, B. Fiedler, K. Schulte, Compos. Sci. Technol. 64 (2004) 2363.

[8] J. Che, T. Cagin, W.A. Goddard, Nanotechnology 11 (2000) 65.

[9] H. Huang, C.H. Liu, Y. Wu, S. Fan, Adv. Mater. 17 (2005) 1652.

[10] M.J. Biercuk, M.C. Llaguno, M. Radosavljevic, J.K. Hyun, A.T. Johnson, Appl. Phys. Lett. 80 (2002) 2767.

[11] E.T. Thostenson, C. Li, T.W. Chou, Compos. Sci. Technol. 65 (2005) 491.

[12] P.G. Collins, K. Bradley, M. Ishigami, A. Zettl, Science 287 (2000) 1801.

[13] P. Giannozzi, R. Car, G. Scoles, J. Chem. Phys. 118 (2003) 1003.

[14] S.A. Babanejad, F. Ashrafi, A. Ghasemi, Arch. Appl. Sci. Res. 2 (2010) 438.

[15] A.A. Rafati, S.M. Hashemianzadeh, Z. Bolboli Nojini, J. Phys. Chem. C. 112 (2008) 3597.

[16] M. Cinke, J. Li, Jr. C.W. Bauschlicher, A. Ricca, M. Meyyappan, Chem. Phys. Lett. 376 (2003) 761.

[17] X. Lu, C. Sun, F. Li, H.M. Cheng, Chem. Phys. Lett. 454 (2008) 305.

[18] J.F. Espinal, A. Montoya, F. Mondragon, T.N. Truong, J. Phys. Chem. B. 108 (2004) 1003.

[19] D. Henwoo, J.D. Carey, Phys. Rev. B 75 (2007) 245413.

[20] K. Azizi, S.M. Hashemianzadeh, S. Bahramifar, Current Applied Physics, 11 (2011) 776.

[21] Yu, SeGi; Whikun Yi, "Single-Walled Carbon Nanotubes as a Chemical Sensor for SO_2 Detection, Nanotechnology, IEEE Transactions on, 6 (2007) 545.

[22] A.C. Lua, T. Yang, Chem. Eng. J. 155 (2009) 175.

[23] X. Zhou, W.Q. Tian, X.L. Wang, Sensor. Actuat. B-Chem. 151 (2010) 56.

[24] F. Yau, D.L. Duong, S.C. Lim, S.B. Yang, H.R. Hwang, W.J. Yu, I.H. Lee, F. Günes, Y.H. Lee, J. Matt. Chem. 21 (2011) 4502.

[25] J. Zhao, A. Buldum, J. Han, J.P. Lu, Nanotechnology 13 (2002) 195.

[26] M. Oftadeh, B. Gholamalian, M. Hamadanian, J. Nanostruct. 1 (2012) 213.

[27] M. Oftadeh, M. Gholamian, H.H. Abdallah, Int. Nano Lett. 3 (2013) 7.

[28] M.J. Frisch, G.W. Trucks, H.B. Schlegel, G.E. Scuseria, M.A. Robb, J.R. Cheeseman, G. Scalmani, V. Barone, B. Mennucci, G.A. Petersson, H. Nakatsuji, M. Caricato, X. Li, H.P. Hratchian, A.F. Izmaylov, J. Bloino, G. Zheng, J.L. Sonnenberg, M. Hada, M. Ehara, K. Toyota, R. Fukuda, J. Hasegawa, M. Ishida, T. Nakajima, Y. Honda, O. Kitao, H. Nakai, T. Vreven, J.A. Montgomery, Jr., J.E. Peralta, F. Ogliaro, M. Bearpark, J.J. Heyd, E. Brothers, K.N. Kudin, V.N. Staroverov, R. Kobayashi, J. Normand, K. Raghavachari, A. Rendell, J.C. Burant, S.S. Iyengar, J. Tomasi, M. Cossi, N. Rega, J.M. Millam, M. Klene, J.E. Knox, J.B. Cross, V. Bakken, C. Adamo, J. Jaramillo, R. Gomperts, R.E. Stratmann, O. Yazyev, A.J. Austin, R. Cammi, C. Pomelli, J.W. Ochterski, R.L. Martin, K. Morokuma, V.G. Zakrzewski, G.A. Voth, P. Salvador, J.J. Dannenberg, S. Dapprich, A.D. Daniels, Ö. Farkas, J.B. Foresman, J.V. Ortiz, J. Cioslowski, D.J. Fox, Gaussian, Inc., Wallingford CT, 2009.

[29] G. Lendvay, I. Mayer, Chem. Phys. Lett. 297 (1998) 365.

[30] A.E. Reed, L.A. Curtiss, F. Weinhold, Chem. Rev. 88 (1988) 899.